Inorg. Chem. **2003**, *42*, 7782–7788

Structure and Bonding of Sr_3In_{11}: How Size and Electronic Effects Determine Structural Stability of Polar Intermetallic Compounds

Shahrad Amerioun and Ulrich Häussermann*

Department of Inorganic Chemistry, Stockholm University, 10691 Stockholm, Sweden

Received June 3, 2003

The binary compound Sr_3In_{11} ($SrIn_{3.667}$) was synthesized and structurally characterized by X-ray diffraction experiments. It crystallizes in the orthorhombic La_3Al_{11} structure type (space group *Immm*, $Z = 2$; $a = 4.9257(6)$, $b = 14.247(2)$, $c = 11.212(2)$ Å). The crystal structure of Sr_3In_{11} bears features of the monoclinic $EuIn_4$ structure, which is adopted by $SrIn_4$, and the prominent tetragonal $BaAl_4$ structure. Sr_3In_{11} is stable until 550 °C. At higher temperatures it decomposes peritectically into $SrIn_2$ and In. Structural stability and bonding properties of Sr_3In_{11} were investigated by first principles calculations and compared to $SrIn_4$ in the monoclinic $EuIn_4$ and the tetragonal $BaAl_4$ structure. All three structures consist of a three-dimensional, polyanionic, network formed by In atoms and Sr cations encapsulated in cages. For the $BaAl_4$-type $SrIn_4$, In–In network bonding is perfectly optimized. In contrast, the networks of $EuIn_4$-type $SrIn_4$ and Sr_3In_{11} appear hypo- and hyperelectronic, respectively. The formation of Sr_3In_{11} with a composition close to 1:4 and the nonexistence of $BaAl_4$-type $SrIn_4$ is explained by a delicate interplay of size and electronic factors governing structural stability in the In-rich part of the Sr–In system.

1. Introduction

Polar intermetallic compounds represent the link between metallic and nonmetallic s−p-bonded materials. They form between active metals (alkali, alkaline earth, or rare earth metals) with the metallic elements from the triel (Al, Ga, In, Tl) and tetrel groups (Sn, Pb), and their systematic exploration in recent years revealed a wealth of novel and peculiar structures.[1−6] The p-elements are formally reduced by the electropositive component and form polyanionic clusters or networks with localized multicenter bonding patterns. Thus, bonding in polar intermetallics is intermediate to that of semiconducting Zintl phases with two-center localized bonding within polyanionic entities and s−p-bonded metallic systems without notable internal charge transfer displaying completely delocalized bonding. As a consequence, structural stability of polar intermetallics is not easily rationalized. The intermediate situation between two bonding types involves a complicated interplay between electronic factors and size and packing effects.

Corbett et al. elaborated on this complex question by exploring binary alkaline earth−triel systems with three-dimensional polyanionic networks. In particular, the Sr−In system afforded two new and interesting case examples. Sr_3In_5[7] and $SrIn_4$[8] both exhibit electron-deficient In networks. The deviation from optimum electron count for In−In network bonding was suggested to be a consequence of optimizing size and packing effects between countercations and their hosting cavities provided by the In network.[7,8] In that respect $SrIn_4$ is especially remarkable. This compound crystallizes in the rarely adopted monoclinic $EuIn_4$ structure type, whereas the large majority of 1:4 alkaline earth−triels compounds realize the simple tetragonal $BaAl_4$ structure type. In this work we report on the new Sr−In compound Sr_3In_{11} with a composition close to 1:4. The structure of this compound bears features of both tetragonal $BaAl_4$ and the monoclinic $EuIn_4$ structures. A stability and bonding analysis of Sr_3In_{11} performed on the basis of first principles calculations strongly corroborates the ideas developed by Corbett. Thus, the Sr−In system appears especially susceptible for

* To whom correspondence should be addressed. E-mail: ulrich@inorg.su.se.

(1) Belin, C.; Tillard-Charbonnel, M. *Prog. Solid State Chem.* **1993**, *22*, 59.
(2) Belin, C.; Tillard-Charbonnel, M. *Coord. Chem. Rev.* **1998**, *180*, 529.
(3) Cordier, G.; Eisenmann, B. In *Chemistry, Structure and Bonding of Zintl Phases and Ions*; Kauzlarich; S., Ed.; VCH: New York, 1996; pp 61−137.
(4) Fässler, T. F.; Hoffmann, S. *Z. Kristallogr.* **1999**, *214*, 722.
(5) Corbett, J. D. *Angew. Chem., Int. Ed.* **2000**, *39*, 670.
(6) Corbett, J. D. In *Chemistry, Structure and Bonding of Zintl Phases and Ions*; Kauzlarich; S., Ed.; VCH: New York, 1996; pp 139−181.
(7) Seo, D. K.; Corbett, J. D. *J. Am. Chem. Soc.* **2001**, *123*, 4512.
(8) Seo, D. K.; Corbett, J. D. *J. Am. Chem. Soc.* **2000**, *122*, 9621.

10.1021/ic0301829 CCC: $25.00
Published on Web 11/07/2003

principal studies concerning structural and phase stability in polar intermetallic compounds.

2. Experimental Section

2.1. Synthesis. The title compound was obtained in an attempt to prepare a high-temperature form of $SrIn_4$ with the tetragonal $BaAl_4$ structure. All materials were handled in an Ar-filled glovebox that had moisture and oxygen levels below 1 ppm. Samples were prepared with an excess of In. Under this condition the solid indide is in equilibrium with an In-richer melt (self-flux condition), which is very favorable for crystal growth. Mixtures of Sr (ABCR, 99.9%) and In (ABCR, 99.999%) with an atomic ratio of 1:8 were loaded into specially prepared stainless steel ampules as described by Boström.[9] These ampules contained the reaction mixture at the bottom and a layer of coarsely crushed quartz glass fixed by a plug of quartz wool at the top. Sealed ampules were put into a quartz wool insulated reaction container made of stainless steel, which was subsequently placed into a furnace. The reaction mixture was first heated to 700 °C for 12 h to ensure complete melting and mixing of the metals. After that, temperature was lowered to a reaction temperature between 300 and 450 °C. According to the reported Sr−In phase diagram,[10] in this temperature range a composition 1:8 corresponds to an equilibrium between melt and the In-richest compound. After a reaction time of 48 h the reaction container was turned upside down into a centrifuge which was operated at 3000 rpm for 3 min. The ampule was opened, and the crystalline product was collected from the top of the quartz wool plug. It displayed a silvery luster and was characterized by powder X-ray diffraction patterns taken on a Guinier powder camera with Cu Kα_1 radiation ($\lambda = 1.540\,562$ Å) and by compositional analysis with the EDX (energy-disperse X-ray) method in a JEOL 820 scanning electron microscope. The average composition of five crystallites was 21.9(5) at. % Sr and 78.1(5) at. % In. Sr_3In_{11} is very sensitive to moisture and decomposes rapidly in air.

2.2. Structure Determination. The lattice parameters of Sr_3In_{11} were obtained from a least-squares refinement of 17 measured and indexed lines in the Guinier powder pattern (Si standard).[11] To ensure proper assignment of the indices the observed lines were compared with the calculated ones[12] using the positional parameters resulting from the structure refinements. A needle-shaped Sr_3In_{11} crystal was picked from the 450 °C synthesis sample and sealed in a capillary. Intensity data was collected at 170 K on a STOE IPDS diffractometer with monochromatic Mo Kα radiation ($\lambda = 0.710\,73$ Å). All data sets were corrected for Lorentz and polarizations effects. Absorption correction was performed by the program X-shape as included in the STOE IPDS software.[13] The space group *Immm* was assigned on the basis of the systematic absences and the statistical analysis of the intensity distributions. Structure determination (direct methods) and refinement (full-matrix least squares on F^2) of Sr_3In_{11} was performed with the program SHELX-97 and revealed two and four fully occupied Sr and In positions, respectively.[14] Some details of the single-crystal data collections and refinements are listed in Table 1. Atomic position parameters and selected interatomic distances are given in Tables 2 and 3. Further details of the crystal structure investigation may be obtained as Supporting Information.

Table 1. X-ray Single-Crystal Refinement Data for Sr_3In_{11}[a]

chem formula	Sr_3In_{11}
lattice params (Å)	$a = 4.9257(6)$
	$b = 14.247(2)$
	$c = 11.212(2)$
V (Å^3)	786.86(19)
space group, Z	*Immm*, 2
T (K)	170
fw	1525.9
λ (Å)	0.710 73
ρ_{calcd} (g/cm^3)	6.51
μ (mm^{-1})	26.08
R_1, wR_2	0.0224, 0.0564

a $R_1 = \sum|F_o| - |F_c|/\sum|F_o|$. $wR_2 = (\sum[w(F_o^2 - F_c^2)^2])/(\sum[w(F_o^2)^2])$, $w = 1/[\sigma^2(F_o^2) + (aP)^2 + bP]$ and $P = (F_o^2 + 2F_c^2)/3$ ($a = 0.031$, $b = 0$). The lattice parameters are obtained from Guinier X-ray powder data (Cu Kα_1, 23 °C, 17 indexed lines).

Table 2. Atomic Coordinates and Isotropic-Equivalent Thermal Displacement Parameters for Sr_3In_{11}

	site	x	y	z	U_{eq}[a]
Sr1	2a	0	0	0	0.0072(3)
Sr2	4g	0	0.3102(1)	0	0.0077(2)
In1	2c	1/2	1/2	0	0.0127(3)
In2	4j	1/2	0	0.6954(1)	0.0108(2)
In3	8l	0	0.3426(1)	0.3726(1)	0.0088(2)
In4	8l	0	0.1475(1)	0.2753(1)	0.0094(2)

[a] U_{eq} is defined as one-third of the trace of the orthogonalized $\mathbf{U}_{ij}$ tensor.

Table 3. Selected Bond Lengths in Sr_3In_{11}[a]

In1−In4	3.281	×4	In4−In3	2.973	×2
In1−In2	3.297	×4	In4−In3	2.985	
			In4−In2	3.254	×2
In2−In3	2.996	×2	In4−In1	3.281	
In2−In4	3.254	×4			
In2−In1	3.297	×2	Sr1−In3	3.624	×8
			Sr1−In4	3.735	×4
In3−In3	2.856				
In3−In4	2.973	×2	Sr2−In2	3.481	×2
In3−In4	2.985		Sr2−In4	3.574	×4
In3−In2	2.996		Sr2−In3	3.583	×4
			Sr2−In1	3.658	×2
			Sr2−In1	3.860	×2

[a] Standard deviations are equal or less than 0.001 Å.

2.3. Electronic Structure Calculations. Total energy calculations for $SrIn_4$ ($BaAl_4$- and $EuIn_4$-types) and Sr_3In_{11} were performed in the framework of the frozen core all-electron projected augmented wave (PAW) method[15] (as implemented in the program VASP[16]). For all systems atomic position parameters and lattice parameters were relaxed for a set of constant volumes until forces had converged to less than 0.01 eV/Å. In a second step, we extracted the equilibrium volume V_0 and its corresponding energy E_0 by fitting the E vs V values to a Birch−Murnaghan equation of state. The exchange and correlation energy was assessed by the generalized gradient approximation (GGA).[17] Convergency of the calculations was checked with respect to the plane wave cutoff and the number of k points used in the summation over the Brillouin zone. Concerning the plane wave cutoff a energy value of 300 eV was

(9) Boström, M.; Hovmöller, S. *J. Solid State Chem.* **2000**, *153*, 398.
(10) Massalski, T. S. *Binary Alloy Phase Diagrams*, 2nd ed.; American Society for Metals: Metals Park, OH, 1990.
(11) Werner, P.-E. *Ark. Kemi* **1969**, *31*, 513.
(12) Yvon, K.; Jeitschko, W.; Parthé, E. *J. Appl. Crystallogr.* **1977**, *10*, 73.
(13) *IPDS*, version 2.87; Stoe and Cie GmbH: Darmstadt, Germany, 1996. *XSHAPE*: *Crystal Optimisation for Numerical Absorption Correction*; Stoe and Cie GmbH: Darmstadt, Germany, 1996.
(14) Sheldrick, G. M. *SHELX97*; University of Göttingen: Göttingen, Germany, 1997.
(15) Blöchl, P. E. *Phys. Rev. B* **1994**, *50*, 17953. Kresse, G.; Joubert, J. *Phys. Rev. B* **1999**, *59*, 1758.
(16) Kresse, G.; Hafner, J. *Phys. Rev. B* **1993**, *47*, RC558. Kresse, G.; Furthmüller, J. *Phys. Rev. B* **1996**, *54*, 11169.
(17) Perdew, J. P.; Wang, Y. *Phys. Rev. B* **1992**, *45*, 13244.

chosen for all systems. *k* points were generated by the Monkhorst−Pack method[18] and sampled on grids of 10 × 10 × 10 (Sr_3In_{11}), 11 × 11 × 11 ($SrIn_4$ ($BaAl_4$)), and 8 × 8 × 8 ($SrIn_4$ ($EuIn_4$)). The integration over the Brillouin zone was performed with a Gaussian smearing of 20 mRy. Total energies were converged to better than 1 meV/atom.

The TB-LMTO method in the atomic sphere approximation[19] was employed to calculate In−In crystal orbital Hamilton populations (COHP)[20] for the three systems. A COHP analysis provides a measure of the bonding character and strength of atomic contacts. The TB-LMTO calculations were performed on the basis of the VASP−PAW relaxed structures. The electronic density of states (DOS) produced by both methods were found to be in good agreement.

3. Results and Discussion

3.1. Comments on the In-Rich Part of the Sr−In Phase Diagram. For the In-rich part of the Sr−In phase diagram the phases $SrIn_5$, $SrIn_3$, Sr_2In_5, and $SrIn_2$ are reported.[10] The former three phases decompose peritectically at 420, 540, and 620 °C, respectively, whereas $SrIn_2$ melts congruently at 930 °C. The applied melt−centrifugation synthesis method presents an excellent tool for screening particular temperature ranges for thermodynamic stable compounds. We obtained monoclinic $SrIn_4$[8] from the 1:8 Sr−In reaction mixtures in a temperature interval between 200 and 425 °C. At 450 °C this reaction mixture yielded Sr_3In_{11}. Thus, it can be safely stated that $SrIn_4$ is the most In-rich compound in the binary system Sr−In. It is stable until 425 + δ °C (δ < 25 K). We proceeded to investigate the In-rich part of the Sr−In phase diagram at higher temperatures. To keep the reaction mixture below the liquidus curve the Sr:In ratio was successively decreased. Reaction mixtures with a composition 1:6 were employed between 450 and 550 °C, mixtures 1:5 between 550 and 600 °C, mixtures 1:4 between 600 and 700 °C, and mixtures 1:3 between 700 and 800 °C. Sr_3In_{11} was found to be stable until 550 + δ °C (δ < 25 K). At higher temperatures this compound is succeeded by $SrIn_2$ ($CaIn_2$ structure type),[21] which was formed at temperatures between 575 and 800 °C. Importantly, there was no indication of the intermediate phases $SrIn_3$ and Sr_2In_5. The temperatures of the peritectic decompositions of $SrIn_5$ and $SrIn_3$ are close to those of $SrIn_4$ and Sr_3In_{11}. Therefore, it is likely that $SrIn_5$ corresponds to $SrIn_4$ and $SrIn_3$ to Sr_3In_{11}.

3.2. Crystal Structure Relationships. Sr_3In_{11} is the first compound with the La_3Al_{11} structure[22] exclusively formed by main group metals. There are about 75 representatives for the La_3Al_{11} type, most of them ternary compounds consisting of a rare earth metal, a transition metal, and either Ga or Al.[23] Binary compounds exist in rare-earth aluminum and rare-earth zinc systems. The structure of Sr_3In_{11} resembles strongly that of tetragonal $BaAl_4$ but also bears

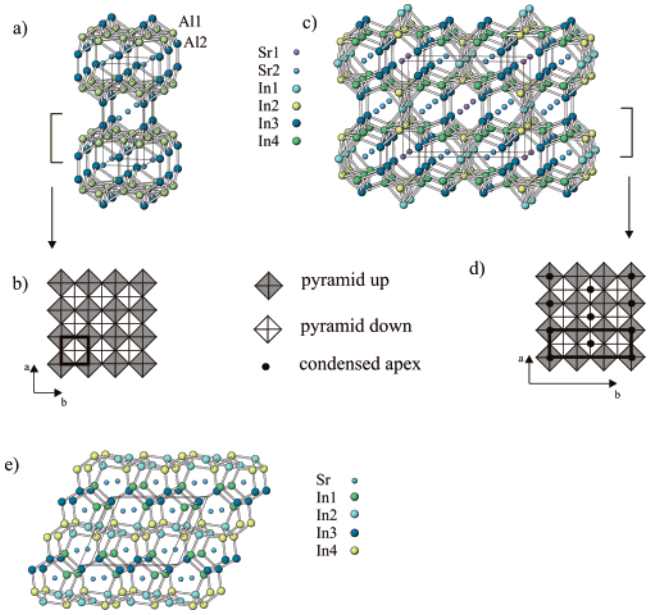

Figure 1. Comparison of the crystal structures of tetragonal $BaAl_4$ (a), orthorhombic Sr_3In_{11} (La_3Al_{11}-type) (c), and monoclinic $SrIn_4$ ($EuIn_4$-type) (e). $BaAl_4$ and Sr_3In_{11} consist of layers of square pyramids. These layers and their connection are shown in (b) and (d), respectively.

features of monoclinic $SrIn_4$ ($EuIn_4$ type). These structural relationships are discussed in the following (Figure 1).

In body-centered tetragonal $BaAl_4$ (space group *I*4/*mmm*) Ba atoms occupy corner and center positions and the Al atoms form a $^3_\infty[Al_4]^{2-}$ network (Figure 1a). This network contains two independent sites: the basal Al (Al1) atoms occupy the Wyckoff site 4d and form two-dimensional square nets which are alternately capped above and below the plane by the apical atoms (Al2) on Wyckoff site 4e. The resulting layers of square pyramids (Figure 1b) are connected between Al2 atoms to yield the final network. Orthorhombic body-centered Sr_3In_{11} (Figure 1c) can be considered as a ordered defect variant of $BaAl_4$.[24,25] The unit cell is three times larger and contains 28 atoms (6 Sr and 22 In). Two of the apical−apical connections have been condensed to single atoms (In1, Figure 1d), which accounts for the deviation from the composition 1:4 (6:24). In Sr_3In_{11} the ratio between apical−apical connections and condensations (defects) is 2:1.[26] The introduction of apical atom defects leads to a disruption of the square nets (i.e. the bases of the square pyramids) which change into ribbons along the *b* axis. These apical atom defects in Sr_3In_{11} have also important consequences for the countercation coordination. In $BaAl_4$ the coordination polyhedron of Ba corresponds to an 18-vertex space-filling Fedorov polyhedron composed of six- and four-membered rings. In La_3Al_{11}-type Sr_3In_{11} Sr1 has a comparable coordina-

(18) Monkhorst, H. J.; Pack, J. D. *Phys. Rev. B* **1972**, *13*, 5188.
(19) Krier, G.; Jepsen, O.; Burkhardt, A.; Andersen, O. K. *The TB-LMTO-ASA Program*, version 4.7; Max-Planck Institut: Stuttgart, Germany, 1997.
(20) Dronskowski, R.; Blöchl, P. E. *J. Phys. Chem.* **1993**, *97*, 8617.
(21) Iandelli, A. *Z. Anorg. Allg. Chem.* **1964**, *330*, 221.
(22) Gomes de Mesquita, A. H.; Buschow, K. H. J. *Acta Crystallogr.* **1967**, *22*, 497.
(23) Villars, P.; Calvert, L. D. *Pearsons Handbook of Crystallographic Data for Intermetallic Compounds*, 2nd ed.; ASM International: Materials Park, OH, 1991. Villars, P.; Calvert, L. D. *Pearsons Handbook of Crystallographic Data for Intermetallic Compounds*, desk ed.; ASM International: Materials Park, OH, 1997
(24) Nordell, K. J.; Miller, G. J. *Angew. Chem., Int. Ed. Engl.* **1997**, *36*, 2008.
(25) Biehl, E.; Deiseroth, H. J. *Z. Anorg. Allg. Chem.* **1999**, *625*, 389.
(26) The recently discovered compound Rb_5Hg_{19} realizes another defect variant of the $BaAl_4$-type with an apical−apical connection-to-defect ratio of 4:1.[25]

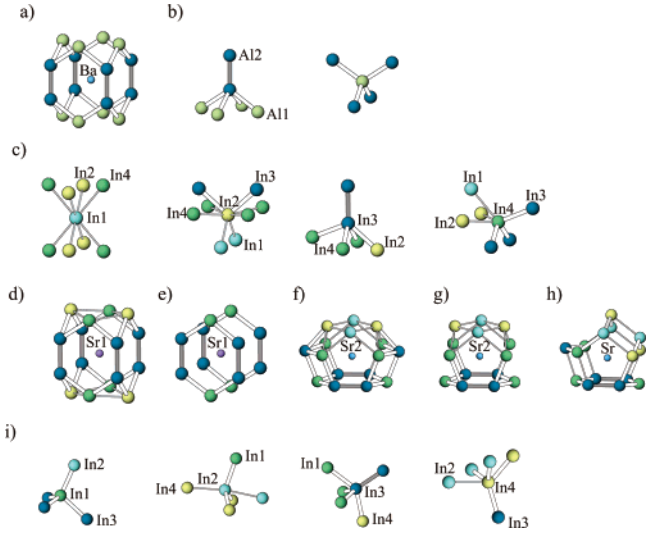

Figure 2. Coordination environment of atoms in the structures of $BaAl_4$, Sr_3In_{11}, and $SrIn_4$: (a) Ba and (b) Al coordination in $BaAl_4$; (c) In coordination in Sr_3In_{11}; (d) extended and (e) actual (<4 Å) coordination of Sr1 in Sr_3In_{11}; (f) extended and (g) actual (<4 Å) coordination of Sr2 in Sr_3In_{11}; (h) Sr coordination in $SrIn_4$; (i) In coordination in $SrIn_4$. The three sets of In−In network distances are indicated: gray bold lines, white bold lines, and thin lines represent short, medium, and long distances, respectively.

tion polyhedron, whereas that of Sr2 features five-membered rings. The Sr2 coordination by In is very similar to that of Sr in monoclinic $SrIn_4$ (Figure 1e).

In the next step we deepen the comparison between the three structures by examining in more detail the local coordination of the network forming atoms and the countercations (Figure 2). We first note that in $BaAl_4$ Ba is rather 16 coordinated by 8 Al1 and 8 Al2 atoms (Figure 2a), since two additional Al2 atoms are distinctly farther away from the center of the Fedorov polyhedron (cf. Figure 1a). Al1 is nearly tetrahedrally surrounded by four Al2 atoms, Al2 is surrounded by four Al1, and one Al2 in a square pyramidal fashion (Figure 2b). According to the bonding description of Zheng and Hoffmann[27] and Burdett and Miller,[28] Al2−Al2 two-center two-electron (2c2e) bonds connect neighboring sheets of square pyramids. The second bonding contact in this network is the distance between Al1 and Al2 atoms yielding localized multicenter (5c6e) bonding in the pyramids $Al2Al1_4$. The distance between two Al1 atoms in the square net is long and considered to be nonbonding. The condensation of apexes in Sr_3In_{11} leads to a square prismatic coordination of In1 by four In2 and four In4 atoms (Figure 2c). The distances of In1 to its nearest neighbors (cf Table 3) compare to those in elemental bct-In (3.25 Å × 4 and 3.38 Å × 8).[29] In3 corresponds to apical Al2 in the $BaAl_4$ structure. Its 1 + 4 coordination is clearly recognizable. In2 and In4 correspond to the basal Al1 atoms. However, their local coordination is increased to 2 + 6 and 3 + 3, respectively. The shorter distances (of about 3.0 Å) involve formally apical In3 atoms, and the longer ones (of about 3.3 Å) involve further In2 and In4 atoms. The latter distances are in the range of nearest neighbor distances in elemental In. This is an important difference to the network of the $BaAl_4$ structure. For all alkaline earth−triel compounds, the interbasal distance (i.e. the distance of the square net) is considerably longer than nearest neighbor distances in the elemental structures of the constituting triels metals. Remarkably, the In−In distances in the Sr_3In_{11} network are distinctively split into three sets (Table 3). The shortest distance of 2.86 Å occurs between two In3 atoms. This is the formally apical−apical connection, which might be associated with a 2c2e bond. The next set of distances (In3−In2, In3−In4) is in the narrow range between 2.97 and 3.0 Å and might be associated with localized multicenter bonding. The third set (In1−In4, In1−In2, In2−In4) between 3.25 and 3.3 Å corresponds to formally interbasal distances. Their distance distribution compares well with that of the nearest-neighbor distances in elemental In and, thus, indicates metallic bonding interaction between the involved atoms.

Next we turn to the countercation coordinations. Sr1 in Sr_3In_{11} corresponds to Ba in $BaAl_4$, which has a 16 atom coordination (Figure 2d). This number, however, appears reduced to 12 atoms (8 × In3 and 4 × In4) for Sr1 (Figure 2e). Figure 2f shows an extended coordination environment for Sr2. Sr2 is sandwiched between two pentagon rings which are connected by a ring of 6 more In atoms which forms a plane with Sr2. Of this 16 atoms only 14 (or rather 12 + 2) can be considered as nearest neighbor coordination for Sr2 (Figure 2g). Interestingly, the Sr2 coordination in Sr_3In_{11} greatly resembles the Sr coordination in monoclinic $SrIn_4$. There, the two In pentagon rings sandwiching Sr are connected by a ring of 5 additional In atoms, which, however, has a quite irregular shape (Figure 2h). Also, the local coordination of the In atoms in $SrIn_4$ bears similarities to Sr_3In_{11} (Figure 2i). In3 can be identified as an apical, 1 + 4 coordinated atom, and In1, as a basal, tetrahedrally coordinated atom. The distances in the In network of $SrIn_4$ show a similar, although not so pronounced, splitting in three sets as in Sr_3In_{11}. The shortest In−In distance (between two In 3 atoms) is 2.85 Å, the next group of distances is in a range of 2.91 to 3.08 Å, and the third set is between 3.28 and 3.32 Å (see ref 8 and the discussion in the next section).

The comparison of the crystal structures of Sr_3In_{11}, $SrIn_4$, and $BaAl_4$ allows some conclusions. In the $BaAl_4$ structure, which has the highest symmetry, network forming atoms and countercations have low and high coordination numbers, respectively. For $SrIn_4$ the $BaAl_4$ structure leads to a size mismatch between the volumes of the countercation and its coordination polyhedron (cage) provided by the In network. This was already stressed by Corbett.[8] However, there is a strong driving force to form a 1:4 compound in the Sr−In system, and there appear two solutions to this dilemma. Instead of realizing the tetragonal $BaAl_4$ structure, $SrIn_4$ adopts the monoclinic $EuIn_4$ structure and, additionally, a slightly In-deficient compound ($SrIn_{3.667}$) with a structure closely related to $BaAl_4$ is formed. Compared to $BaAl_4$, in the structures of $SrIn_4$ and Sr_3In_{11} the coordination number of the Sr atoms is lowered (i.e. the size of their coordination polyhedra is decreased) and in turn the coordination number

(27) Zeng, C.; Hoffmann, R. *Z. Naturfosch.* **1986**, *41b*, 292.
(28) Burdett, J. K.; Miller, G. J. *Chem. Mater.* **1990**, *2*, 12.
(29) Donohue, J. *The Structures of the Elements*; Wiley: New York, 1974.

Table 4. Calculated Lattice Parameters and Formation Enthalpies ($\Delta H_f = E(Sr_mIn_n) - (m \times E(Sr) + n \times E(In))$) for $SrIn_4$ ($BaAl_4$- and $EuIn_4$-Types) and Sr_3In_{11}[a]

	$SrIn_4$ ($BaAl_4$): tetragonal	Sr_3In_{11}: orthorhombic	$SrIn_4$ ($EuIn_4$): monoclinic
V (Å^3)	298.25	815.86	582.18
		786.82	*557.2*
a (Å)	4.9393	4.9688	12.1265
		4.9257	*12.079*
b (Å)		14.4068	5.2787
		14.247	*5.1245*
c (Å)	12.2251	11.3971	10.0346
		11.212	*9.920*
β (deg)			114.99
			114.85
ΔH_f (eV/atom)	−0.291	−0.328	−0.306

[a] Experimental values are given in italics ($SrIn_4$ ($EuIn_4$), ref 8).

Table 5. Selected Calculated Distances (Å) in $SrIn_4$ ($BaAl_4$- and $EuIn_4$-Types) and Sr_3In_{11} ($d < 4$ Å)[a]

$SrIn_4$ ($BaAl_4$)		Sr_3In_{11}		$SrIn_4$ ($EuIn_4$)	
In1−In2	2.98 × 4	In1−In4	3.32 (3.28) × 4	In1−In2	2.98 (2.93)
In1−In1	3.51 × 4	In1−In2	3.33 (3.30) × 4	In1−In3	2.99 (2.93) × 2
				In1−In3	3.10 (3.08)
In2−In2	2.80	In2−In3	3.05 (3.00) × 2		
In2−In1	2.98 × 4	In2−In4	3.28 (3.25) × 4	In2−In1	2.98 (2.93)
		In2−In1	3.33 (3.30) × 2	In2−In4	3.00 (2.94) × 2
Sr−In2	3.77 × 8			In2−In4	3.27 (3.28)
Sr−In1	3.94 × 8	In3−In3	2.90 (2.86)	In2−In2	3.35 (3.32)
		In3−In4	3.01 (2.97) × 2		
		In3−In4	3.03 (2.99)	In3−In3	2.89 (2.85)
		In3−In2	3.05 (3.00)	In3−In4	2.96 (2.91)
				In3−In1	2.99 (2.93)
		In4−In3	3.01 (2.97) × 2	In3−In1	3.10 (3.08)
		In4−In3	3.03 (2.99)		
		In4−In2	3.28 (3.25) × 2	In4−In3	2.96 (2.91)
		In4−In1	3.32 (3.28)	In4−In2	3.00 (2.94) × 2
				In4−In4	3.05 (3.00)
		Sr1−In3	3.66 (3.62) × 8	In4−In2	3.27 (3.28)
		Sr1−In4	3.79 (3.74) × 4		
				Sr−In2	3.52 (3.50)
		Sr2−In2	3.52 (3.48) × 2	Sr−In1	3.55 (3.51)
		Sr2−In4	3.62 (3.57) × 4	Sr−In2	3.63 (3.56) × 2
		Sr2−In3	3.62 (3.58) × 4	Sr−In1	3.64 (3.57) × 2
		Sr2−In1	3.69 (3.66) × 2	Sr−In3	3.66 (3.64) × 2
		Sr2−In4	3.93 (3.86) × 2	Sr−In1	3.71 (3.66)
				Sr−In3	3.75 (3.68) × 2
				Sr−In4	3.76 (3.68) × 2
				Sr−In3	3.86 (3.86)
				Sr−In4	3.90 (3.89)

[a] Experimental values are given in parentheses ($SrIn_4$ ($EuIn_4$), ref 8).

of the In atoms is increased. This introduces new, longer, In−In network distances, which compare to those in elemental In. In the following, we attempt to put these considerations on a more quantitative basis.

3.3. Electronic Structure and Bonding Relationships. We performed first principles density functional calculations to investigate structure and phase competition in the In-rich part of the Sr−In system and to analyze electronic structure and bonding properties of the compounds $SrIn_4$ and Sr_3In_{11}. The results of the computational structure optimization are summarized in Tables 4 and 5. An additional table is given as Supporting Information. For Sr_3In_{11} the experimental structural parameters are well reproduced, and for $SrIn_4$ the deviations are somewhat larger. The theoretical equilibrium volume for both compounds is overestimated by about 4%. The overestimation of ground state volumes is frequently observed when using GGA for assessing exchange and correlation energy. For Sr_3In_{11} the calculated energy of formation (enthalpy of formation at 0 K) is by 0.022 eV/atom larger than that for $EuIn_4$-type $SrIn_4$. This difference is also reflected in the higher thermal stability of the former compound. The energy difference between $SrIn_4$ in the monoclinic $EuIn_4$ and in the hypothetical tetragonal $BaAl_4$ structure is 0.075 eV/Z or 7.5 kJ/mol. For the reaction $3 \times SrIn_4$ ($BaAl_4$) → Sr_3In_{11} + In we obtain a negative enthalpy (referring to 0 K). Thus, in accord with our experimental results, $SrIn_4$ does not realize a high-temperature form with the higher symmetry $BaAl_4$ structure. Instead, the formation of slightly In-deficient Sr_3In_{11} is preferred. The volume/formula unit of $SrIn_4$ is by 2.5% larger in the $BaAl_4$ than in the $EuIn_4$ structure. This strongly supports the idea that structure selection depends on size effects, because in the more condensed $EuIn_4$ structure Sr should be more effectively coordinated.

First principles calculation allow one to study compounds in hypothetical structures. It is instructive to have a closer look at $SrIn_4$ with the important $BaAl_4$-type structure. In Table 5 we compare interatomic distances in $SrIn_4$ ($BaAl_4$ and $EuIn_4$ structures) and in Sr_3In_{11}. Calculated interatomic distances deviate by 1−2% from the experimental ones for Sr_3In_{11}- and $EuIn_4$-type $SrIn_4$. In $BaAl_4$-type $SrIn_4$ the short apical−apical contact in the In network, which is associated with a 2c2e bond, is 2.8 Å. The apical−basal (In2−In1) distance within the multicenter-bonded pyramids is 2.98 Å. The interbasal distance (In1−In1) within the square nets is 3.51 Å and thus considerably longer than the nearest-neighbor distances in elemental In (3.25 Å × 4 and 3.38 Å × 8). The apical−apical and apical−basal distances in $SrIn_4$ with the hypothetical $BaAl_4$ structure are important indicators for the other structures since they are connected with a well-understood bonding picture developed for this structure type.[27,28] Indeed, as already discussed, distances in $EuIn_4$-type $SrIn_4$ and Sr_3In_{11} group around 2.85, 3.0, and 3.3 Å. The In−In distance distribution in $BaAl_4$-type $SrIn_4$ justifies the assignment of localized 2c2e and multicenter bonding for the first and second set of distances, respectively, in $EuIn_4$-type $SrIn_4$ and Sr_3In_{11}; i.e., both compounds bear bonding features of the $BaAl_4$ type. In $BaAl_4$-type $SrIn_4$ Sr is coordinated by 16 In atoms at distances between 3.8 and 3.9 Å. In the two lower symmetry structures Sr is coordinated by fewer In atoms and Sr−In distances are significantly shorter.

The electronic density of states (DOS) of the three Sr−In compounds are assembled in Figure 3. Most conspicuously, the DOS of $BaAl_4$-type $SrIn_4$ exhibits a pronounced pseudogap at the Fermi level. The features of this pseudogap are considerably diminished for Sr_3In_{11}- and $EuIn_4$-type $SrIn_4$. The contribution of Sr states is rather low below the Fermi level and drastically increasing above. This behavior is typical for polar intermetallic compounds and Zintl phases, which formally are composed of an oxidized electropositive component (the active metal) and a polyanionic (reduced) network. Although the overall shape of the DOS curves is

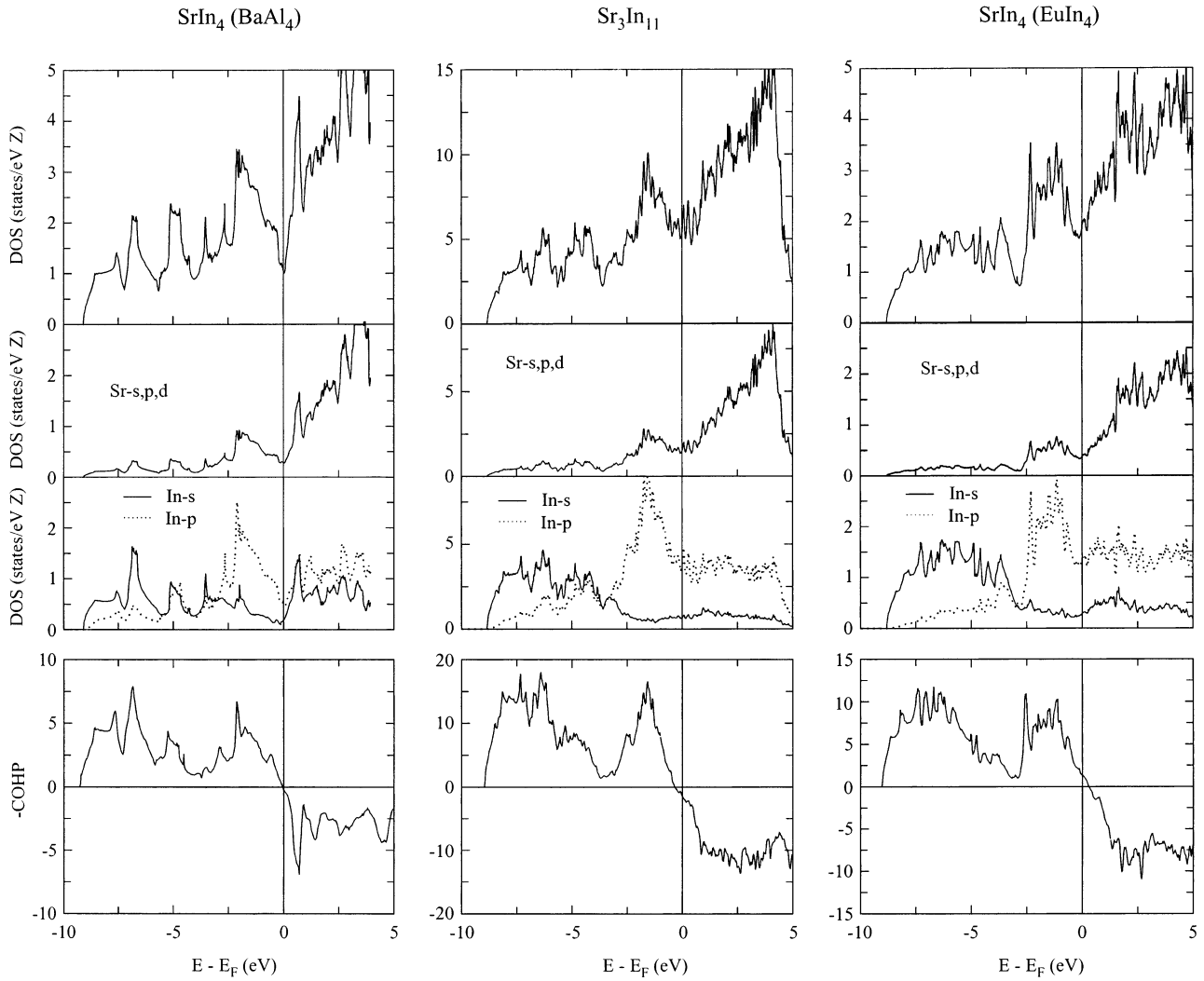

Figure 3. Total DOS (top panel) and partial DOS (middle panels) of the Sr and In sites for the systems $SrIn_4$ ($BaAl_4$), Sr_3In_{11}, and $SrIn_4$ ($EuIn_4$) calculated at the theoretical equilibrium volume. The In states are divided into s- and p-orbital contributions. The bottom panel shows −COHP summed for all In−In network contacts in the unit cell below 4 Å for each system. Positive values of −COHP indicate bonding and negative antibonding character. The Fermi level E_F is set to zero.

similar, the distribution of s- and p-based In bands is different for the three compounds. For $BaAl_4$-type $SrIn_4$ we observe a pronounced s−p mixing, whereas for $EuIn_4$-type $SrIn_4$ In s and p bands are markedly separated. For Sr_3In_{11} the situation is intermediate. The analysis of the COHP reveals that the Fermi level (and thus the pseudogap) in $BaAl_4$-type $SrIn_4$ sharply and exactly separates In−In bonding from antibonding states. Thus, In−In bonding in this network appears most effectively optimized. In contrast, the In networks in $EuIn_4$-type $SrIn_4$ and Sr_3In_{11} are hypo- and hyperelectronic, respectively. As already pointed out by Corbett, the optimum electron count for $EuIn_4$-type $SrIn_4$ to fill all In−In bonding levels would be 15 electrons/formula unit (i.e. one electron more than in $SrIn_4$).[8] For La_3Al_{11}-type Sr_3In_{11} the electron count for optimum In−In bonding would be 38 electrons/formula unit (i.e. one electron less than in Sr_3In_{11}). According to Nordell and Miller, this optimum electron count is achieved in ternary derivatives of the La_3Al_{11} type (e.g. $Dy_3Au_2Al_9$).[24] Conclusively, structural stability of compounds in the In-rich part of the Sr−In system is not exclusively determined by optimizing In−In network bonding. The requirement of size match between Sr and the cavities provided by the In network leads to small deviations from optimum electron count for In−In network bonding in $SrIn_4$, Sr_3In_{11}, and Sr_3In_5.

We conclude this section by inspecting the integrated COHP (ICOHP) values for the In−In contacts occurring in the computationally relaxed structures of $SrIn_4$ and Sr_3In_{11}. This is shown in Figure 4. In the distance range of 2.8−3.4 Å ICOHP values vary approximately linearly. When using the apical−apical (2c2e bonded) distance of 2.8 Å in $BaAl_4$-type $SrIn_4$ as a reference, a bond order scale for In−In distances can be established. According to this scale, the shortest In−In contacts in $EuIn_4$-type $SrIn_4$ and Sr_3In_{11} obtain bond orders of 0.85−0.9. Multicenter bonded and metallic bonded In−In contacts obtain bond orders around 0.6 and 0.35, respectively. These two types of contacts are well separated in $EuIn_4$-type $SrIn_4$ and Sr_3In_{11} by about 0.2 Å. The ICOHP (and bond order) values of the In−In nearest neighbor contacts in elemental bct-In coincide with those of the long In network distances in $EuIn_4$-type $SrIn_4$ and Sr_3In_{11}.

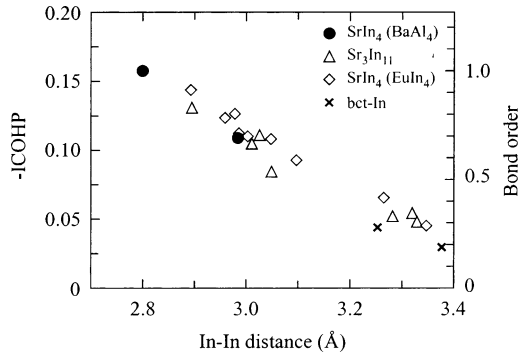

Figure 4. Distribution of the energy-integrated −COHP (−ICOHP) values for the In−In network contacts below 3.5 Å occurring in the structures of $BaAl_4$-type $SrIn_4$ (black circles), Sr_3In_{11} (triangles), $EuAl_4$-type $SrIn_4$ (diamonds), and elemental In (crosses). The right-hand side of the graph shows an In−In bond order scale based on the shortest network distance as a reference.

4. Conclusions

We reported on the new polar intermetallic compound Sr_3In_{11} which is the first representative of the La_3Al_{11} structure exclusively formed by main group metals. The crystal structure of Sr_3In_{11} resembles that of the $BaAl_4$ and $EuIn_4$ structure types with a three-dimensional polyanionic In network encapsulating Sr counterions. As in Sr_3In_5[7] and $SrIn_4$,[8] In−In network bonding in Sr_3In_{11} is not completely optimized. From the results of first principles calculations we conclude that the formation of Sr_3In_{11} stems from the strong endeavor of the Sr−In system to form a 1:4 compound. The great majority of alkaline earth−triel systems display such a compound with the $BaAl_4$ structure. In this structure triel−triel network bonding is perfectly optimized. On the other side, the rather rigid high-symmetry $BaAl_4$ structure implies a size mismatch between the Sr and the cavities provided by the surrounding In network. This size mismatch is countered flexibly by the Sr−In system with the realization of the lower symmetry $EuIn_4$ structure for $SrIn_4$ and the formation of Sr_3In_{11} crystallizing with a defect variant of the $BaAl_4$ structure.

Acknowledgment. This work was supported by the Swedish Research Council (VR).

Note Added in Proof. Recently, we became aware of a work by J.-G. Mao and A. M. Guloy who also reported on the crystal structure and bonding properties of Sr_3In_{11}.[30] Their result of the crystal structure determination is virtually identical to ours. For assessing the electronic structure of Sr_3In_{11} Mao and Guloy used semiempirical extended-Hückel band structure calculations while we employed a first principles method. We arrive at a somewhat different conclusion concerning the bonding properties of this compound.

Supporting Information Available: One X-ray crystallographic file in CIF format and one table containing the computationally obtained positional parameters of $SrIn_4$ ($BaAl_4$- and $EuIn_4$-types) and Sr_3In_{11}. This material is available free of charge via the Internet at http://pubs.acs.org.

IC0301829

(30) Mao, J.-G.; Guloy, A. M. *J. Alloys Compds.* **2003**, in press.